Sensors and Actuators B 267 (2018) 34–41

Contents lists available at ScienceDirect

Sensors and Actuators B: Chemical

journal homepage: www.elsevier.com/locate/snb

# A "cleanroom-free" and scalable manufacturing technology for the microfluidic generation of lipid-stabilized droplets and cell-sized multisomes

Tatiana Trantidou [a,*], Anna Regoutz [b], Xian N. Voon [a], David J. Payne [b], Oscar Ces [a,c,*]

[a] Department of Chemistry, Imperial College London, Exhibition Road, South Kensington, SW7 2AZ, UK
[b] Department of Materials, Imperial College London, Exhibition Road, South Kensington, SW7 2AZ, UK
[c] Institute of Chemical Biology, Imperial College London, Exhibition Road, South Kensington, SW7 2AZ, UK

ARTICLE INFO

*Article history:*
Received 1 February 2018
Received in revised form 23 March 2018
Accepted 27 March 2018
Available online 28 March 2018

*Keywords:*
Droplet microfluidics
Artificial cells
Lipid droplets
Double emulsions
Rapid prototyping
Scalable manufacturing

ABSTRACT

There is a growing demand to construct artificial biomimetic structures from the bottom-up using simple chemical components in a controlled and high-throughput way. These cell mimics are encapsulated by lipid membranes and can reconstitute biological machinery within them. To date, such synthetic cells based upon droplet microfluidics are fabricated using non-scalable, expensive and time-consuming strategies, and are thus restricted to small-scale in-house manufacturing. Here, we report a "cleanroom-free" and highly scalable microfluidic manufacturing technology based on dry film resists and multilayer lamination. The technology facilitates the controlled and high-throughput generation of stable and monodisperse droplets using anionic surfactants and more biologically relevant phospholipids. We demonstrate the versatility of this approach by selectively patterning the surface chemistry of the device, enabling the production of compartmentalized lipid structures based on droplet interface bilayers (multisomes). This technology has the potential to simultaneously unlock the widespread exploitation of microfluidics to chemists and synthetic biologists not having access to controlled production environments and facilitate low-cost (<£1) high-volume fabrication of self-contained disposable devices with minimum feature sizes of 30 μm. The associated material and equipment costs approach those of other deskilled prototyping technologies, such as 3D printing that have made the transition into the mainstream.



## 1. Introduction

Lipid-stabilized droplets and double emulsions (termed multisomes) comprise the building blocks of artificial cells. These advanced micro- and nanosized biomimetic systems have been leveraged to date in a wide range of applications; as cell models for studying fundamental biology [1,2], chemical microreactors able to produce their own enzymes [3], therapeutic delivery vehicles capable of on-board chemical synthesis [4], and as artificial cells that perform specific operations and interact with neighboring biological or synthetic cells [5]. In the next decade, industrial scale-up of cell-free systems is expected to facilitate and accelerate the production of high-value and high-volume chemicals that is currently performed using cell-based methods and is thus restricted by the complexity of physiological systems, cell growth and cell viability [6].

Droplet microfluidics have certainly scaled up the production of these synthetic cells over the last decade. To date, microfluidic device fabrication for artificial cell generation is dominated by polydimethylsiloxane (PDMS)-based devices made via soft-lithography [7–14]. PDMS offers the advantages of biocompatibility, optical transparency and compatibility with organic solvents, nevertheless, the process requires the use of centralized microfabrication facilities for the production of Si masters via conventional photolithography. Therefore, it involves high costs in terms of facilities and materials (photoresists) and is a time-consuming process. Most importantly, the fabrication technology is not scalable, therefore, it is limited to small-scale in-house manufacturing. Furthermore, the material's tendency to rapidly recover its native surface hydrophobicity (water contact angle >100°) after standard surface treatments (e.g. plasma oxidation or UV irradiation), requires subsequent coating with charged anions and cations [7] or hydrophilic molecules [8,9,14] to facilitate the formation of oil-in water (o/w) droplets.

* Corresponding authors at: Department of Chemistry, Imperial College London, Exhibition Road, South Kensington, SW7 2AZ, UK.
*E-mail addresses:* t.trantidou@imperial.ac.uk (T. Trantidou), o.ces@imperial.ac.uk (O. Ces).

https://doi.org/10.1016/j.snb.2018.03.165
0925-4005/

Glass capillaries are less widely employed for lipid systems assembly [15–19]; these are readily purchased and are reusable, but their set-up and manipulation is primarily done manually. There are also a few other manufacturing technologies, such as Si-based devices produced by wet etching [20]. Glass and Si micromachining via wet etching is traditionally the oldest and most widely known manufacturing technology for microfluidic devices, however, it is an expensive and time-consuming process, and requires the use of cleanroom suites. Application of these devices in microfluidic droplet generation requires the use of hydrophobic coatings to favor water-in oil (w/o) droplet formation, which often degrade with multiple uses.

Rapid prototyping and the production of a small series of identical devices are often key requirements for microfluidic applications in research laboratories. On the other hand, a fully scalable fabrication technology which enables mass production of microfluidic devices at a low cost has the potential to change the landscape of microfluidics, and establish low-cost high-end devices available both for research and industrial use. In this work, we introduce and characterize a fabrication process for *segmented flow* microfluidics based on biocompatible permanent dry film resists (DFR) and multi-layer lamination, and we showcase application of this technology in the emerging field of bottom-up synthetic biology. DFR are photosensitive polymers that are crosslinked under UV light and have been initially introduced for Printed Circuit Board (PCB) fabrication. To date, DFR have been employed to interface electronics with *continuous flow* microfluidics [21,22], as negative mold templates for fabricating microfluidic devices via hot embossing [23,24], PDMS mold casting [25,26] and wet etching [27], and as sealing layers of plastic microfluidic devices fabricated via injection molding [28].

Here, we showcase for the first time the use of DFR in droplet-based microfluidics and in particular their application in the construction of biomimetic artificial membranes. The microfluidic formation of lipid-stabilized droplets remains the most challenging type of droplet generation, since there is a very specific favorable wettability between the liquids, the lipids and the channel materials to facilitate microfluidic droplet generation. The proposed technology comprises a simple, elegant, economical and unique in its flexibility method for the automatic and high-throughput production of droplets and double emulsions using both anionic surfactants and more biologically relevant phospholipids for artificial cell chassis fabrication, outperforming current methods in terms of scalability, cost, time and convenience. The manufacturing process is ideal for low-cost rapid prototyping of microfluidic devices, as it does not require cleanroom facilities and is solely based on two low-cost pieces of equipment; an office laminator and a UV lamp. Moreover, it is compatible with fabrication flowcharts in major industrial facilities, therefore, the technology can be scaled up to achieve mass production of microfluidic devices for synthetic biology applications. We also demonstrate a versatile technique to permanently modify specific regions of the microfluidic device to create microchannels with defined surface wettability characteristics, and further demonstrate this in the generation of more complex multiple emulsion systems. This technique is far more advantageous compared to a variety of surface modification methods for other materials (e.g. PDMS) in terms of simplicity, convenience, longevity and robustness.

## 2. Experimental section

### 2.1. Microfluidic device fabrication

Poly(methyl methacrylate) (PMMA) thin sheets (Weatherall Ltd, Wendover, UK) were used as support substrates. The microfluidic inlets/outlets were created using a bench drill or a laser cutter. The samples were thoroughly cleaned dried and dehydrated. The acrylic pieces were laminated with a 55 μm-thick dry film resist (Ordyl SY355) from Mega Electronics Ltd (Cambridge, UK) using an office laminator (A3 Mega Drive laminator, Mega Electonics Ltd). To create access to the reservoirs, the laminated substrates were exposed to UV light via a transparency film mask using a collimated UV mercury lamp as the light source. The substrates were baked on a hotplate at 85 °C for 5 min. The resist was developed in Ordyl SY300 Developer followed by immersion and rigorous shaking into the Ordyl SY300 Rinse (Mega Electonics Ltd). The substrates were then laminated with a second sheet of dry film resist. Depending on the desired microfluidic channel depth, multiple laminations were performed. The substrates were exposed to UV light to create the microfluidic channels as previously described. The microfluidic substrates were sealed via lamination with a 55 μm-thick sheet of Ordyl. Finally, NanoPorts (IDEX, London, UK) were glued using an epoxy resin on top of the inlets.

For o/w droplet generation the sealing and microfluidic substrates were exposed to oxygen plasma (Femto UHP, Diener Electronic GmbH, Ebhausen, Germany) to create a hydrophilic microfluidic channel network. For lipid-stabilized droplet generation further hydrophilic treatment was necessary, which was achieved through flushing 1 wt% polyvinyl alcohol (PVA) (Sigma Aldrich, Dorset, UK) in Milli-Q water through the channels. The solution was then removed and the device was dehydrated (110 °C, 15 min). The process was repeated thrice.

For generating surfactant-stabilized w/o/w double emulsions, the microfluidic device was designed and fabricated with two flow focusing junctions. Before sealing the device, the channels were selectively exposed to oxygen plasma. For lipid-stabilized w/o/w emulsions, the same process was performed for the sealing substrates, followed by sealing via lamination and then selective treatment with PVA; air was flushed into the channels that were to remain hydrophobic, while the PVA solution was flushed into the hydrophilic channels. The solution was then removed and the device was baked (110 °C, 15 min). This process was repeated thrice.

### 2.2. Preparation of solutions for droplet and double emulsion generation

Lipid powder was purchased from Avanti Polar Lipids (Alabaster, AL, USA). The powder was predissolved in chloroform (Sigma Aldrich) which was removed under a stream of nitrogen to give a lipid film. Oil was then added, and the mixtures were sonicated for 15 min to fully dissolve the lipid.

### 2.3. Static contact angle and interfacial tension measurements

Contact angle and interfacial tension (IFT) measurements were performed using a Drop Shape Analyzer DSA100 (Krüss GmbH, Bristol, UK). Water-in-air contact angles were extrapolated using the circle fitting method. Water-in-oil contact angles were extrapolated using a macro in ImageJ (NIH, Bethesda, MD, USA) [29]. IFT values were extrapolated using the available built-in software for the automatic calculation of IFT based on iterative fitting of the Young–Laplace equation.

### 2.4. X-ray photoelectron spectroscopy (XPS)

The spectra were recorded on a Thermo Scientific K-Alpha+ X-ray Photoelectron Spectrometer system, incorporating a monochromated, micro-focused Al Kα X-ray source ($h\nu$ = 1486.6 eV) and a 180° double focusing hemispherical analyzer with two-dimensional detector. The X-ray source was operated at 6 mA emission current and 12 kV anode bias. Data were collected

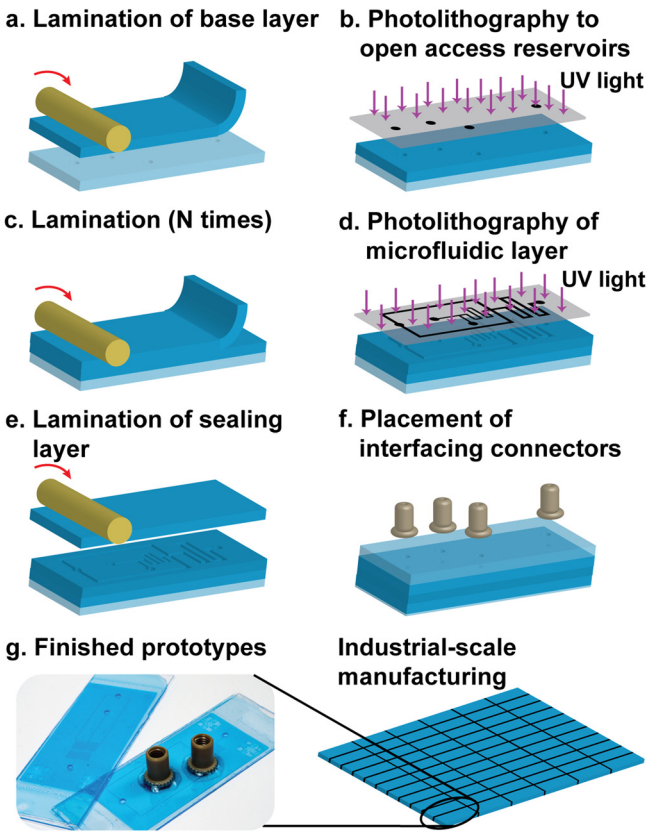


**Fig. 1.** Microfluidic device fabrication. (a) A DFR sheet is laminated on an acrylic sheet using lamination rolls. (b) The film is exposed to UV light via a transparency film mask. (c) Multiple laminations occur based on the desired channel depth. (d) The film(s) are exposed to UV light to pattern the microfluidic channels. (e) A final DFR lamination is performed to seal the device. (f) Interfacing connectors are placed on the inlets and outlets. (g) Prototyped microfluidic devices that can also be mass-manufactured.

using a 400 μm X-ray spot and a pass energy of 200 eV for survey and 20 eV for core level spectra.

## 3. Results and discussion

### 3.1. Microfluidic device

For the fabrication of the microfluidic device, we employed a DFR (Ordyl SY300) which is highly biocompatible and optically transparent, can achieve good resolution/feature sizes, and is low-cost comparatively to other commercially available DFR; currently the price per square meter for Ordyl SY300 (55 μm thick) is £58.7/m$^2$ as opposed to £90.7/m$^2$ for TMMF S2000 – TOK, and £276.9/m$^2$ for DF-1000 – EMS of similar thicknesses. Ordyl dry film resist is available in a range of thicknesses (17 μm, 20 μm, 30 μm and 55 μm) and the deviation in thickness is as low as 0.01% [30], which is extremely difficult to achieve with photoresists in conventional spin coating processes. The proposed fabrication method is ideal for low-cost, rapid, "cleanroom-free" prototyping of microfluidic devices, as it only requires a standard office laminator and a UV light source, maintaining the overall cost for necessary equipment significantly low.

The fabrication process of the microfluidic devices and the finished prototypes are illustrated in Fig. 1. The manufacturing process is characterized by low-cost materials and low material consumption, keeping the cost of each microfluidic device at approximately ~£1 per device. It is worth mentioning that the interfacing connectors can be easily removed from the acrylic surface before disposing of the microfluidic device, cleaned and reused.

Ordyl is natively hydrophobic with a water contact angle of ~75° (Fig. S1), which makes the material ideal for manufacturing microfluidic devices dedicated to w/o droplet generation. In the case that the microfluidic device is intended for o/w droplet generation, which is essential for the production of multiple emulsions, an extra step precedes the final sealing, which entails modification of the desired flow focusing junction via plasma oxidation. This technique is far more advantageous compared to a variety of surface modification methods for other materials; for example, plasma oxidation of PDMS is only temporary and the material's native hydrophobicity is fully restored within an hour after treatment [31], while layer-by-layer deposition of hydrophilic coatings to glass and PDMS [32] is complex, time-consuming and degrades with multiple uses. In contrast, the hydrophilic modification of the DFR using plasma oxidation can be accurately controlled based on the process parameters (plasma power and exposure time), achieving superhydrophilic surfaces (water contact angle <1°) with a long-lasting irreversible effect (Fig. S1). This also facilitates the production of devices that can serve as off-the-shelf components that can be manufactured and stored long term for future use.

The proposed method is a simple and affordable solution for the production of multiple microfluidic devices that can be fabricated simultaneously in less than an hour. With automation, the fabrication yield can be significantly accelerated with tens of microfluidic devices fabricated in a single go. DFR can be easily laminated onto any kind of substrate in a large area due to its unique structure, thus the proposed strategy is also suitable for mass-production of high-end microfluidic devices in order to accelerate their commercial exploitation.

### 3.2. Microfluidic droplet generation

The microfluidic devices were first tested for the generation of w/o droplets using anionic surfactants (0.1 wt% Span-80 in mineral oil and 0.5 wt% SDS in water) (Fig. S2), but focus in this study was placed on the generation of lipid-stabilized w/o droplets as a synthetic biology exemplar. We used a biologically relevant lipid, DOPC (1,2-dioleoyl-sn-glycero-3-phosphocholine) in squalene (10 mg ml$^{-1}$). Microfluidic devices were manufactured with a flow focusing junction (Fig. 2a). Based on the selected DFR thickness (17 or 55 μm) and the number of laminated layers, flow focusing junctions of different geometries were fabricated (34 × 30 μm, 55 × 50 μm and 110 × 100 μm) and droplets were generated with equivalent sizes to the channel geometries. It is noteworthy that the selected DFR can be photolithographically patterned with an aspect ratio of 1:1, i.e. the minimum channel dimensions that can be achieved are approximately 20 μm in width using a 17 μm-thick DFR. Therefore, the minimum channel dimensions that can be achieved using this technology are around 17 × 20 μm.

The ability to further control droplet size by altering the degree of lipid focusing through adjustment of the applied flow rate ratio (FRR) at a 110 × 100 μm flow focusing junction is depicted in Fig. 2b. FRR is defined as the lipid/oil volumetric flow rate divided by the aqueous volumetric flow rate. As expected, modal diameter of the microfluidic-generated lipid droplets was observed to scale inversely with FRR [33,34] and this was valid for all devices regardless of the aspect ratio, with a minimum modal diameter of 16.41 ± 1.7 μm (N = 77) achieved with a flow focusing junction of cross section 34 × 30 and FRR 1.5 (Fig. S3). In all cases, the microfluidic devices were able to sustain high flow rates ( > 100 μl min$^{-1}$ for the external oil phase) without compromising the device sealing.

The size distributions of lipid droplets with varying FRR were also compared using a device with a 110 × 100 μm flow focusing junction (Fig. 2c). To quantify the monodispersity of the generated

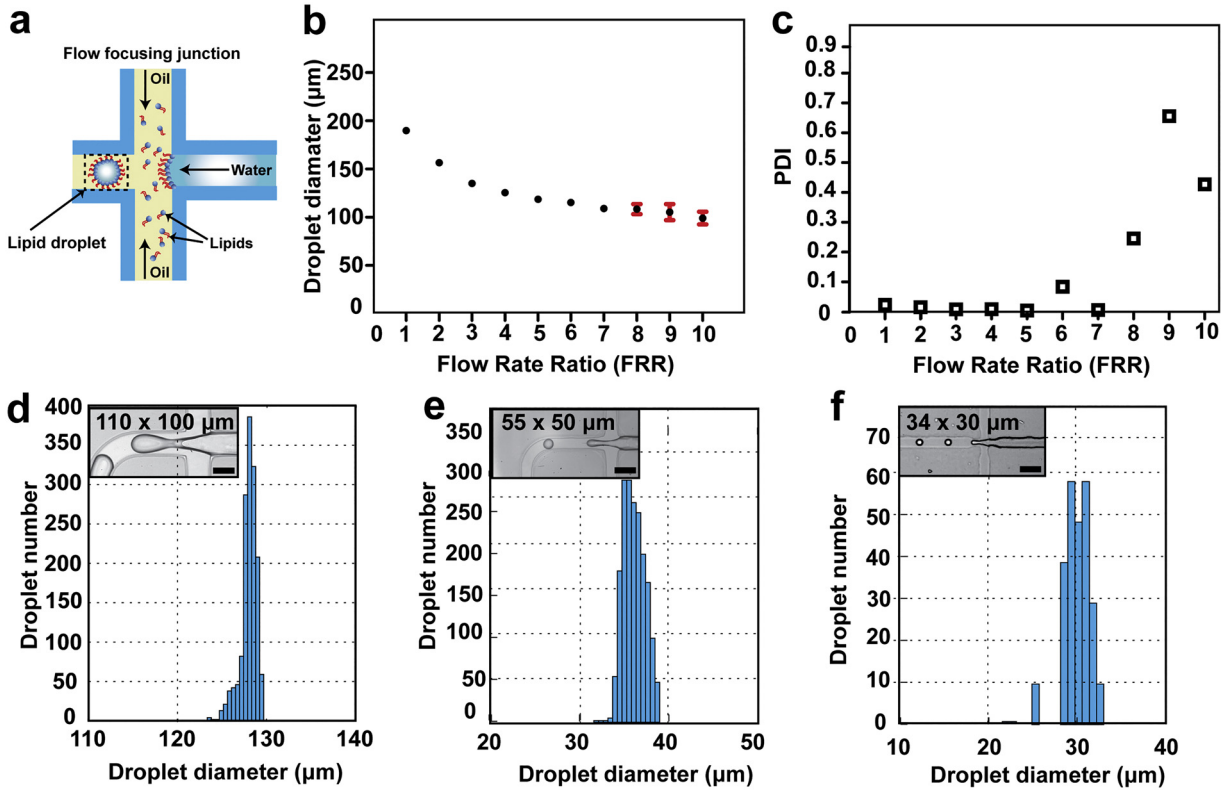


**Fig. 2.** (a) Schematic representation of droplet formation in a flow focusing junction. (b) Modal diameter of lipid droplets produced within a DFR device with a channel cross section 110 × 100 μm. Error bars are shown in red and correspond to the standard deviation (SD) for >700 droplets. (c) Polydispersity index (PDI) of each droplet sample produced within a DFR device. (d)-(f) Size distributions of lipid droplets formed within DFR devices of cross sections (d) 110 × 100 μm, (e) 55 × 50 μm and (f) 34 × 30 μm. FRR for these data are 2, 2.5 and 1 respectively. Scale bars in (d)-(f) 100 μm. (For interpretation of the references to colour in this figure legend, the reader is referred to the web version of this article.)

droplets, we used a dimensionless parameter, the polydispersity index (PDI), which in the case of a droplet population with a Gaussian size distribution is given by the square of the standard deviation of the distribution divided by the mean size. Low polydispersity (PDI <0.1) was maintained for all FRRs studied, although an increasing trend in PDI was observed for FRR values above 8. This was primarily attributed to the presence of instabilities in the disperse water flow due to the high flow rate of the external oil phase. Comparisons between the population of lipid droplets generated through all three device types reveal that all devices produced narrowly distributed populations of droplets (Fig. 2d-f).

### 3.3. Characterization of lipid-stabilized droplets

Droplet generation in a microfluidic junction is affected by characteristics of the channels such as surface wettability and charge, and material properties including fluid viscosities, surfactant type, and concentration, among others [35]. We investigated the effect of different DOPC concentrations to assess the effect of lipid concentration on the microfluidic droplet formation. Five different DOPC concentration regimes were tested (1, 2, 5, 10 and 20 mg ml$^{-1}$ DOPC in squalene) (Fig. 3a). We observed that the droplet formation mechanism differed with varying lipid concentration. Between 1 and 5 mg ml$^{-1}$, the disperse water phase severely wetted the microfluidic channel and broke into droplets further down the flow focusing junction. At higher concentrations ( < 10 mg ml$^{-1}$), droplet breakup occurred consistently at the flow focusing junction. In addition, the modular diameter of the droplets was considerably smaller at higher concentrations.

It has been previously reported that the stability of microfluidic droplet generation using anionic surfactants critically depends on the preferential wetting of the microchannel walls by the disperse phase [36]. In this study, we hypothesized that the lipid concentration, acting as a biological surfactant, would affect droplet production in a similar way. We investigated how the material interfaces with distinct lipid concentrations immediately and in the long term by performing a series of contact angle measurements of lipid-stabilized droplets sitting on a DFR substrate inside a lipid/oil solution We used 0.5 μl water droplets to neglect the gravitational effect on the measurements. Initial (t = 0) contact angle of lipid-stabilized water droplets increased with increasing DOPC concentration (1 and 20 mg ml$^{-1}$ of DOPC in squalene) (Fig. 3b) and this difference was maintained throughout the first 15 min until all droplets reached equilibrium (Fig. S4). Within the 15 min time interval, equilibrium was reached only for the highest DOPC concentration (20 mg ml$^{-1}$) yet 1 min after formation of the droplet in the oil environment. Based on the surface area of a single DOPC lipid (0.67–0.69 nm$^2$) [37] and the surface of a 0.5 μl droplet used in this study ($3.14 \cdot 10^{12}$ nm$^2$), in all conditions there is an abundance of lipids to achieve equilibrium even for the lowest concentrations (see Table S1).

It is noteworthy that contact angles at t = 0 best represent the dynamic behavior of droplet formation in a microfluidic device. The "bean shape" was immediately prominent at higher DOPC concentrations (Fig. 3b). This was primarily attributed to the interfacial tension (IFT) force which tends to minimize the contact area of the droplet with the DFR substrate according to the thermodynamic principle of minimum interfacial energy. Similar to surfactants, at high lipid concentrations IFT between water and oil is significantly

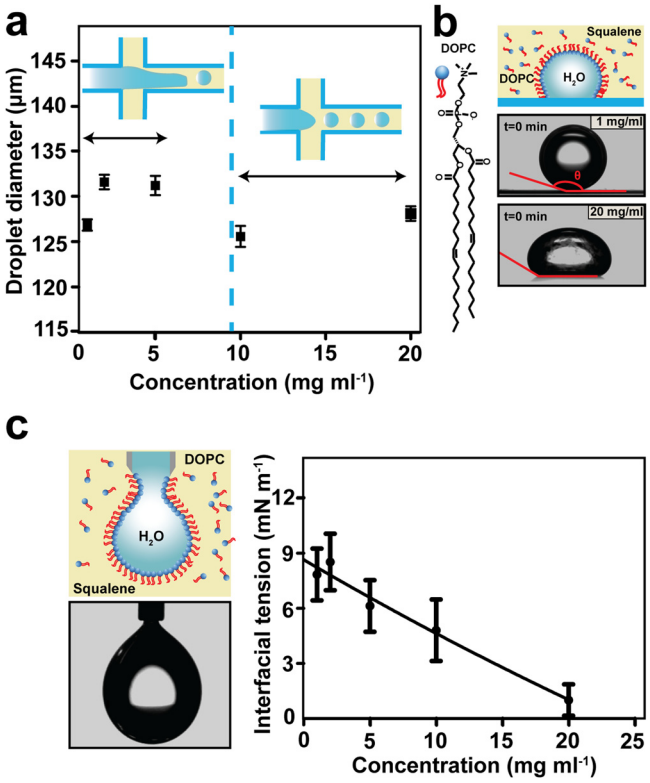


**Fig. 3.** (a) Droplet modal diameter as a function of concentration of DOPC in squalene, indicating different droplet formation regimes at fixed flow rates (2 and 8 μl min$^{-1}$ for the aqueous and lipid/oil phase, respectively. N = 1000 independent droplets). (b) Schematic drawing and real images of sessile w/o droplets on a DFR substrate. (c) dynamic IFT as a function of DOPC concentration (N = 3 independent samples). Droplet size and IFT data are shown with error bars of the standard deviation (SD).

low, thus gravity becomes the dominant force that pulls the droplet down and accounts for the bean shape.

Furthermore, we conducted a series of IFT experiments using pendent water droplets in a lipid/oil environment. The measurement setup of a pendent drop used for profile analysis tensiometry is visualized in Fig. 3c and an idealized lipid monolayer is illustrated in the same figure. The IFT values for all lipid concentrations over time were extrapolated using iterative fitting of the Young-Laplace equation that balances gravitational deformation of the drop with the restorative IFT. In all cases, the maximum possible droplet volume was used in order to reach equilibrium before the droplet pinches off the syringe, ensuring high measurement precision [38]. Fig. 3c also shows the dynamic IFT values at time point zero $\gamma=\gamma(0)$ for each case. Higher lipid concentrations resulted in a dramatic decrease of IFT ($1.01 \pm 0.85$ mN m$^{-1}$ for 20 mg ml$^{-1}$ DOPC as opposed to $7.84 \pm 1.41$ mN m$^{-1}$ for 1 mg ml$^{-1}$). The IFT values at equilibrium ($\gamma e$) for each case are presented in Table S2 for comparison.

Although it is evident from our data that lipid concentration affects the level of wetting on the DFR surface, the significant differences in IFT that arise from the distinct lipid concentrations indicate that IFT is the driving force that determines the flow wetting pattern and droplet breakup mechanism during microfluidic droplet generation [39,40]. As a result, a lower capillary number is produced. Previous studies demonstrated that as surfactant concentration increases, interfacial tension becomes more dominant in a two-phase flow and stabilizes the droplet flow with no partial wetting by the aqueous phase, resulting in the generation of smaller droplets [41]. In this study, lipids serve as the biological surfactant which facilitates passive droplet generation via dripping mode [35]. This mode of breakup comes from the capillary instability (Rayleigh-Plateau) and is a result of the competition between inertial and viscous forces that act to deform the liquid interface, and interfacial tension that resists the deformation.

### 3.4. Microfluidic generation of double emulsions

The production of w/o droplets in a microfluidic device requires a junction with hydrophobic surface properties, whereas the production of o/w droplets requires a junction with a hydrophilic surface. In this work, we exposed the DFR surface to oxygen plasma to modify the material's hydrophobic surface. Plasma oxidation has been employed so far to enable bonding of PDMS-based microfluidic chips and has also been combined with hydrophilic coatings to permanently change the hydrophobic properties of PDMS and render the microchannels hydrophilic [8,14].

Plasma oxidation of the microfluidic channels before the final sealing step rendered permanently hydrophilic DFR channels with the ability to seamlessly generate surfactant-stabilized monodisperse o/w droplets (Fig. S2c-d). By tuning the process parameters (plasma power and exposure duration), different levels of hydrophilicity on the DFR microfluidic channels can be achieved. For surfactant-stabilized droplet generation, this surface modification process is simple, quick, robust and long-lasting, as microfluidic devices can be modified and stored in standard room conditions for more than 30 days without compromising their ability to generate monodisperse droplets (Fig. S2e).

Microfluidic generation of lipid-stabilized o/w droplets requires very specific surface chemistries and many surface modification techniques are incompatible with lipids. In this study, we coated the plasma oxidized DFR microfluidic channels with PVA to render the material compatible for microfluidic generation of o/w lipid droplets. The procedure involved plasma oxidation of both the microfluidic and sealing layers, lamination of the two layers together, and subsequently flowing a solution of 1 wt% PVA (87–90% hydrolysis degree) in Milli-Q water through the microchannels for 10 min to enable adsorption on the activated DFR surfaces. The solution was then removed from the channels via blowing dry with a nitrogen stream and the device was dehydrated on a hotplate. The process was repeated overall three times to achieve maximum adsorption of the PVA on the DFR surface, and was proved to be particularly robust with both an immediate and long-term effect (Fig. S5).

For the production of double emulsions, we developed a method to precisely pattern the surface chemistry within a network of microchannels. We leveraged the microfluidic device shown in Fig. 4a, which consists of two sequential flow focusing junctions with different cross sections for droplet generation; a hydrophobic junction to first generate w/o droplets and then a hydrophilic junction of double width to encapsulate these in larger oil droplets. The selective patterning process is simple and quick; half of the device is covered by a piece of PDMS during plasma oxidation to protect the material's native hydrophobicity. The device is then sealed and can be further treated with PVA for the microfluidic generation of lipid-stabilized droplets. Fig. 4a illustrates micrographs of the generated droplets and multisomes at different parts of the microfluidic device. For this experiment, we synthesized multisomes using a binary mixture of DOPC and a negatively charged lipid (DOPG, 1,2-dioleoyl-sn-glycero-3-[phosphorac-(1'-glycerol)])) to showcase compatibility of our technology with various lipid types. 722 double emulsions were generated per minute using 0.5, 5 and 25 μl min$^{-1}$ flow rates for the internal aqueous, middle oil and external aqueous solutions. Throughput can be further increased using higher flow rates for the distinct phases, however, at high flow rates synchronization of the droplet formation frequencies becomes more challenging. To increase visibility,

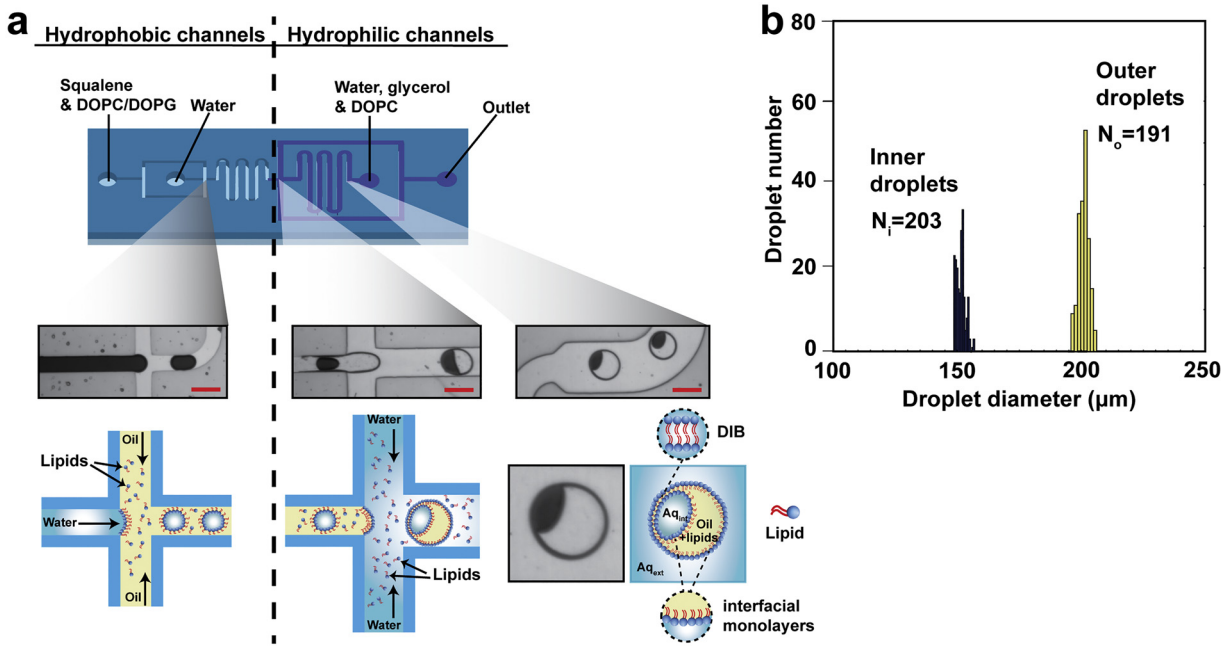


**Fig. 4.** (a) W/o/w double emulsion generation on a selectively treated DFR microfluidic device. Multisomes were produced at flow rates of 0.5, 5 and 25 μl min$^{-1}$ respectively. The middle oil phase consisted of 10 mg ml$^{-1}$ DOPC/DOPG (90:10 molar ratio) in squalene, and the external aqueous phase consisted of 10 mg ml$^{-1}$ DOPC in water with 14% v/v glycerol. The depth of the channels was 100 μm. Scale bars 200 μm. (b) Size distribution of inner and outer droplets shows a high level of droplet monodispersity.

the internal water phase was dyed with 5 mg ml$^{-1}$ Methyl Blue dye. A lipid bilayer was formed at the point of contact between the internal water droplet and the external oil droplet.

The droplet diameter distribution of both the inner water and outer oil droplets was particularly narrow (Fig. 4b); the average diameter for the water droplets was 151.43 μm with a PDI of 0.02 (N = 203 droplets) and the average diameter for the oil droplets was 200.54 μm with a PDI of 0.03 (N = 191 droplets).

### 3.5. Characterization of the material's surface properties

To further characterize the effect of plasma oxidation on the DFR surface, we conducted a series of X-ray Photoelectron Spectroscopy (XPS) experiments. Fig. 5a shows the survey spectra for an untreated DFR surface and three plasma oxidized DFR surfaces using varying process power and time. All major core and Auger lines could be identified. The main contributions from the DFR are C and O with a small amount of N. To investigate changes in the surface chemistry, high resolution spectra of the principal core levels of these three elements were collected (Fig. 5b-d). The C 1 s spectrum for all samples shows three resolved features at 284.5 eV (aliphatic C), 286.1 eV (C—O and C—N), and 288.6 (O—C═O). After plasma treatment the two higher binding energy (BE) features increase in intensity as expected due to the reaction of the oxygen plasma with the DFR surface. This is further supported by an overall increase in the O 1 s spectrum, which shows two features assigned to —OH and ═O environments. In addition to the obvious increase in O, a small reduction in the N present is observed for samples treated at higher plasma power (100). From peak fits to the core levels, relative atomic ratios of C:N:O on the samples' surfaces could be determined, which are summarized in Table S3.

Fig. 5e-h demonstrate representative 10 μl water drops on untreated and plasma oxidized DFR surfaces. The initial water-air contact angle for untreated DFR surfaces was 73.85 ± 4.7° (N = 8) and significantly decreased after plasma oxidation to 14.9 ± 3.0° (N = 2) at 50 W for 1 min, 7.5 ± 1.3° (N = 2) at 100 W for 1 min and 1.35 ± 0.1° (N = 2) at 100 W for 5 min. The reduction in contact angle can be explained by the increase in oxygen-containing species observed in XPS for all conditions, which leads to hydrophilization of the DFR surface. The differences in the magnitude of this reduction are clearly related to changes in the oxygen content, with more aggressive plasma oxidation treatments (high power and/or longer duration) resulting to superhydrophilic DFR surfaces. The alcoholic hydroxyls (C—OH) and carboxylic acids (COOH) generated on the DFR surface after treatment form covalent bonds with the PVA molecules to render the DFR microfluidic devices compatible with o/w droplet generation.

## 4. Conclusions

In this work, we presented a simple and economical technology for the rapid fabrication of microfluidic devices dedicated to artificial cell chassis fabrication. These devices were used for the highly efficient generation of stable and monodisperse w/o and o/w droplets using both anionic surfactants and more biologically relevant phospholipids. A versatile and robust method to selectively pattern the surface chemistry of the device was also achieved using plasma oxidation and subsequent hydrophilic coating of the microfluidic channels via PVA. This enabled the high-throughput production of lipid-stabilized double emulsions (multisomes), which can be further scaled up by increasing the flow rates of the water and oil phases. The developed technology is also ideal for simple and low-cost mass-manufacturing of microfluidic devices for synthetic biology applications. The versatility, robustness, scalability and simplicity of this manufacturing approach has the potential to facilitate the production of biomimetic soft matter devices in high-throughput, moving away from the benchtop and further accelerating the development of double emulsion-based technologies. These soft matter devices have already shown high potential in academia and industry in applications such as the gradual release of pharmaceutical and functional food cargoes [42], the engineering of vesicles for drug delivery [18] and the production of small molecules [7].

Declarations of interest: none.

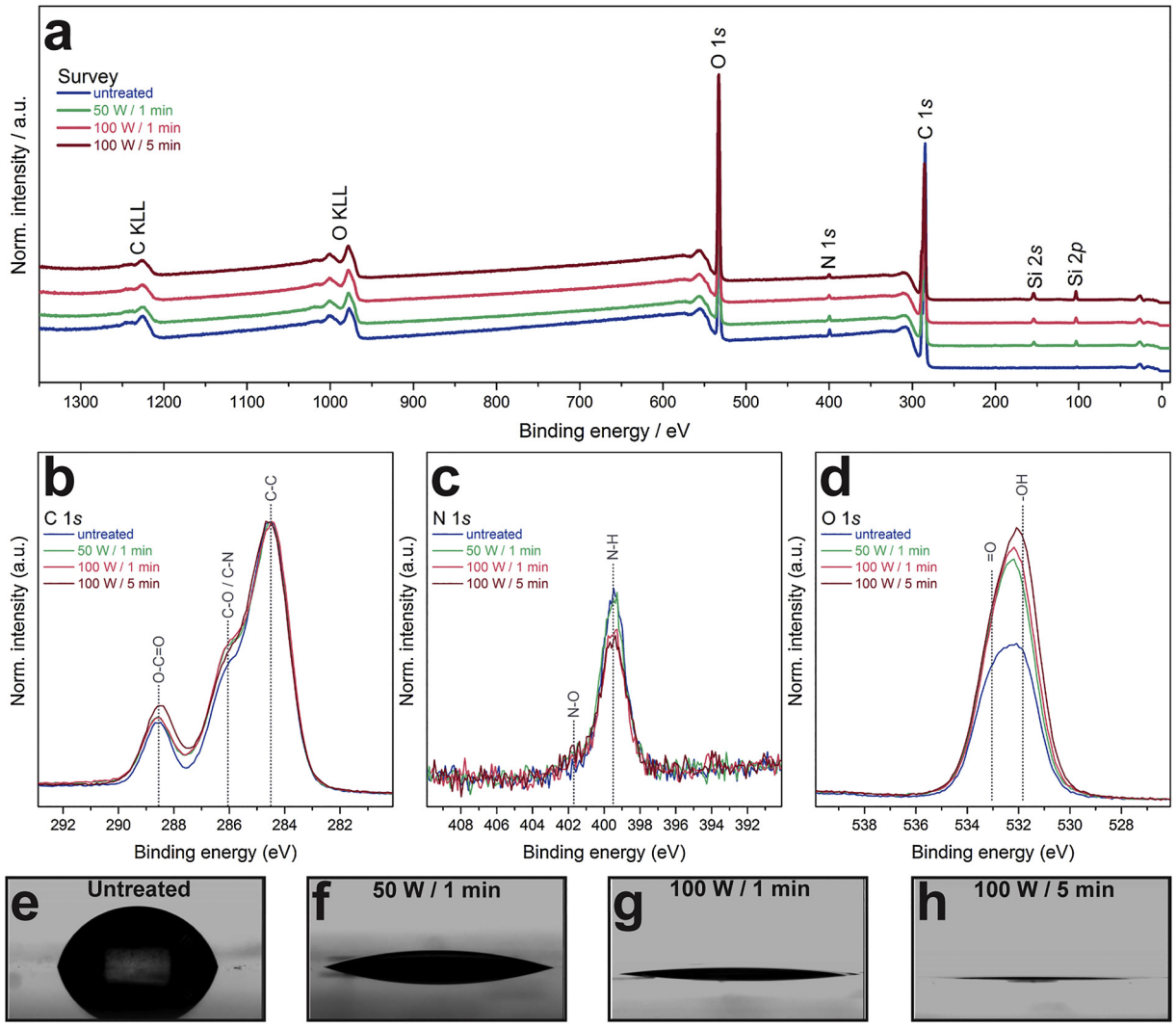


**Fig. 5.** (a) Survey spectrum, (b-d) C, N, and O 1 s core level spectra, (e-h) Representative contact angle images of 10 μl water drops on DFR surfaces: (e) untreated, (f) plasma oxidized at 50 W/1 min, (g) plasma oxidized at 100 W/1 min, (h) plasma oxidized at 100 W/5 min.

## Acknowledgments

This work was supported by the Engineering and Physical Sciences Research Council (EPSRC grant EP/K038648/1). We thank Dr Guido Bolognesi for the python script for the droplet size measurements.

## Appendix A. Supplementary data

Supplementary data associated with this article can be found, in the online version, at https://doi.org/10.1016/j.snb.2018.03.165.

## References

[1] E. Sackmann, A.S. Smith, Physics of cell adhesion: some lessons from cell-mimetic systems, Soft Matter 10 (2014) 1644–1659.
[2] S.H. Tan, B. Semin, J.C. Baret, Microfluidic flow-focusing in ac electric fields, Lab Chip 14 (2014) 1099–1106.
[3] Y. Elani, R.V. Law, O. Ces, Vesicle-based artificial cells as chemical microreactors with spatially segregated reaction pathways, Nat. Commun. 5 (2014) 5305.
[4] H. Daraee, A. Etemadi, M. Kouhi, S. Alimirzalu, A. Akbarzadeh, Application of liposomes in medicine and drug delivery, Artif. Cells Nanomed. Biotechnol. 44 (2016) 381–391.
[5] P.M. Gardner, K. Winzer, B.G. Davis, Sugar synthesis in a protocellular model leads to a cell signaling response in bacteria, Nat. Chem. 1 (2009) 377–383.
[6] C. Schmidt-Dannert, F.J. Lopez-Gallego, A roadmap for biocatalysis-functional and spatial orchestration of enzyme cascades, J. Microb. Biotechnol. 9 (2016) 601–609.
[7] Y. Elani, X.C.I. Solvas, J.B. Edel, R.V. Law, O. Ces, Microfluidic generation of encapsulated droplet interface bilayer networks (multisomes) and their use as cell-like reactors, Chem. Commun. 52 (2016) 5961–5964.
[8] S.Y. Teh, R. Khnouf, H. Fan, A.P. Lee, Stable, biocompatible lipid vesicle generation by solvent extraction-based droplet microfluidics, Biomicrofluidics 5 (2011) 44113.
[9] K. Karamdad, R.V. Law, J.M. Seddon, N.J. Brooks, O. Ces, Preparation and mechanical characterisation of giant unilamellar vesicles by a microfluidic method, Lab Chip 15 (2015) 557–562.
[10] L. Lu, R.M. Irwin, M.A. Coloma, J.W. Schertzer, P.R. Chiarot, Removal of excess interfacial material from surface-modified emulsions using a microfluidic device with triangular post geometry, Microfluid. Nanofluid. 18 (2014) 1233–1246.
[11] L. Lu, J.W. Schertzer, P.R. Chiarot, Continuous microfluidic fabrication of synthetic asymmetric vesicles, Lab Chip 15 (2015) 3591–3599.
[12] S. Matosevic, B.M. Paegel, Stepwise synthesis of giant unilamellar vesicles on a microfluidic assembly line, J. Am. Chem. Soc. 133 (2011) 2798–2800.
[13] S. Matosevic, B.M. Paegel, Layer-by-layer cell membrane assembly, Nat. Chem. 5 (2013) 958–963.
[14] T. Trantidou, Y. Elani, E. Parsons, O. Ces, Hydrophilic surface modification of PDMS for droplet microfluidics using a simple, quick, and robust method via PVA deposition, Microsys. Nanoeng. 3 (2017) 16091.
[15] C.E. Stanley, K.S. Elvira, X.Z. Niu, A. Gee, O. Ces, J.B. Edel, A.J. deMello, A microfluidic approach for high-throughput droplet interface bilayer (DIB) formation, Chem. Commun. (Camb) 46 (2010) 1620–1622.
[16] Y. Elani, A.J. deMello, X. Niu, O. Ces, Novel technologies for the formation of 2-D and 3-D droplet interface bilayer networks, Lab Chip 12 (2012) 3514–3520.

[17] D.K. Baxani, A.J. Morgan, W.D. Jamieson, C.J. Allender, D.A. Barrow, O.K. Castell, Bilayer networks within a hydrogel shell: a Robust chassis for artificial cells and a platform for membrane studies, Angewandte Chemie 128 (2016) 14452–14457.
[18] H.C. Shum, D. Lee, I. Yoon, T. Kodger, D.A. Weitz, Double emulsion templated monodisperse phospholipid vesicles, Langmuir 24 (2008) 7651–7653.
[19] J.C. Stachowiak, D.L. Richmond, T.H. Li, A.P. Liu, S.H. Parekh, D.A. Fletcher, Unilamellar vesicle formation and encapsulation by microfluidic jetting, Proc. Nat. Acad. Sci. U. S. A. 105 (2008) 4697–4702.
[20] A. Jahn, W.N. Vreeland, M. Gaitan, L.E. Locascio, Controlled vesicle self-assembly in microfluidic channels with hydrodynamic focusing, J. Am. Chem. Soc. 126 (2004) 2674–2675.
[21] N. Wangler, L. Gutzweiler, K. Kalkandjiev, C. Müller, F. Mayenfels, H. Reinecke, R. Zengerle, N. Paust, High-resolution permanent photoresist laminate TMMF for sealed microfluidic structures in biological applications, J. Micromech. Microeng. 21 (2011) 095009.
[22] D. Moschou, N. Vourdas, G. Kokkoris, G. Papadakis, J. Parthenios, S. Chatzandroulis, A. Tserepi, All-plastic, low-power, disposable, continuous-flow PCR chip with integrated microheaters for rapid DNA amplification, Sens. Actuators B 199 (2014) 470–478.
[23] P.W. Leech, N. Wu, Y. Zhu, Application of dry film resist in the fabrication of microfluidic chips for droplet generation, Micromech. Microeng. 19 (2009) 065019.
[24] M.E. Sandison, H. Morgan, Rapid fabrication of polymer microfluidic systems for the production of artificial lipid bilayers, J. Micromech. Microeng. 15 (2005) S139.
[25] D. Paul, L. Saias, J.C. Pedinotti, M. Chabert, S. Magnifico, A. Pallandre, B. De Lambert, C. Houdayer, B. Brugg, J.M. Peyrin, J.L. Viovy, A dry and wet hybrid lithography technique for multilevel replication templates: applications to microfluidic neuron culture and two-phase global mixing, Biomicrofluidics 5 (2011) 24102.
[26] K. Stephan, P. Pittet, L. Renaud, P. Kleimann, P. Morin, N. Ouaini, R. Ferrigno, Fast prototyping using a dry film photoresist: microfabrication of soft-lithography masters for microfluidic structures, J. Micromech. Microeng. 17 (2007) N69.
[27] L. Zhang, W. Wang, X.-J. Ju, R. Xie, Z. Liu, L.-Y. Chu, Fabrication of glass-based microfluidic devices with dry film photoresists as pattern transfer masks for wet etching, RSC Adv. 5 (2015) 5638–5646.
[28] L. El Fissi, D. Vandormael, L.A. Francis, Direct assembly of cyclic olefin copolymer microfluidic devices helped by dry photoresist, Sens. Actuators, A 223 (2015) 76–83.
[29] A. Stalder, G. Kulik, D. Sage, L. Barbieri, P. Hoffmann, A snake-based approach to accurate determination of both contact points and contact angles, Colloids Surf. A Physicochem. Eng. Asp. 286 (2006) 92–103.
[30] U. Stöhr, A. Dohse, P. Hoppe, M. Thomas, K. Kadel, C.P. Klages, H. Reinecke, Multilayer photoresist stamps for selective plasma treatment in micrometer scales, Plasma Processes Polym. 6 (2009) 228–233.
[31] T.Y. Chang, V.G. Yadav, S. De Leo, S.A. Mohedas, B. Rajalingam, C.L. Chen, S. Selvarasah, M.R. Dokmeci, A. Khademhosseini, Cell and protein compatibility of parylene-C surfaces, Langmuir 23 (2007) 11718–11725.
[32] W.A. Bauer, M. Fischlechner, C. Abell, W.T. Huck, Hydrophilic PDMS microchannels for high-throughput formation of oil-in-water microdroplets and water-in-oil-in-water double emulsions, Lab Chip 10 (2010) 1814–1819.
[33] A. Jahn, S.M. Stavis, J.S. Hong, W.N. Vreeland, D.L. DeVoe, M. Gaitan, Microfluidic mixing and the formation of nanoscale lipid vesicles, ACS Nano 4 (2010) 2077–2087.
[34] A. Jahn, W.N. Vreeland, D.L. DeVoe, L.E. Locascio, M. Gaitan, Microfluidic directed formation of liposomes of controlled size, Langmuir 23 (2007) 6289–6293.
[35] P. Zhu, L. Wang, Passive and active droplet generation with microfluidics: a review, Lab Chip 17 (2016) 34–75.
[36] W. Li, Z. Nie, H. Zhang, C. Paquet, M. Seo, P. Garstecki, E. Kumacheva, Screening of the effect of surface energy of microchannels on microfluidic emulsification, Langmuir 23 (2007) 8010–8014.
[37] E. Chibowski, A. Szcześ, Zeta potential and surface charge of DPPC and DOPC liposomes in the presence of PLC enzyme, Adsorption 22 (2016) 755–765.
[38] J.D. Berry, M.J. Neeson, R.R. Dagastine, D.Y. Chan, R.F. Tabor, Measurement of surface and interfacial tension using pendant drop tensiometry, J. Colloid Interface Sci. 454 (2015) 226–237.
[39] J. Tan, J.H. Xu, S.W. Li, G.S. Luo, Drop dispenser in a cross-junction microfluidic device: scaling and mechanism of break-up, Chem. Eng. J. 136 (2008) 306–311.
[40] C.P. Tostado, J. Xu, G. Luo, The effects of hydrophilic surfactant concentration and flow ratio on dynamic wetting in a T-junction microfluidic device, Chem. Eng. J. 171 (2011) 1340–1347.
[41] R. Dreyfus, P. Tabeling, H. Willaime, Ordered and disordered patterns in two-phase flows in microchannels, Phys. Rev. Lett. 90 (2003) 144505.
[42] N. Garti, C. Bisperink, Double emulsions: progress and applications, Curr. Opin. Colloid Interface Sci. 3 (1998) 657–667.

## Biographies

**Tatiana Trantidou** obtained her PhD (2014) in biomedical electronics from Imperial College London, UK. At present, she is a research fellow at the Department of Chemistry, Imperial College London, UK. Her research interests are on conventional and unconventional micro/nanofabrication technologies for tissue engineering and for micro/nanofluidics for synthetic biology applications.

**Anna Regoutz** received her PhD (2014) in Inorganic Chemistry from the University of Oxford, UK. At present, she is an Imperial College Research Fellow in the Department of Materials, Imperial College London, UK. Her focus lies on advanced spectroscopy methods for bulk materials, and surfaces and interfaces in functional oxides, particularly for electronic device applications.

**Xian Ning Voon** is a Bachelor Degree student at the Department of Chemistry, Imperial College London, UK. Her research interest is on characterization of materials and microfluidic technologies for artificial cell chassis fabrication.

**David J. Payne** received his M.Chem. (2004) from Cardiff University and DPhil (2008) in experimental solid-state chemistry from the University of Oxford, UK. From 2007 he was a Junior Research Fellow at Christ Church, University of Oxford. At present, he is a Reader and Royal Society University Research Fellow, at the Department of Materials, Imperial College London, UK. His research focuses on the determination of the electronic structure of oxide materials using photoelectron spectroscopy, and in particular developing (lab-based) high pressure X-ray photoelectron spectroscopy (HPXPS). His broader interests in oxide materials focus on energy applications including solid oxide fuel cells, photovoltaics and transparent conducting oxides.

**Oscar Ces** is currently a professor at the Department of Chemistry (Imperial College London, UK), Director of the Institute of Chemical Biology (ICB) and the ICB Centre for Doctoral Training, Director of Development (Chemistry), Co-founder of the EPSRC Frontiers Engineering Program, Co-Director of Fabricell (pan-London Institute focusing on development of novel technologies for artificial cell construction), Co-Director of the Membrane Biophysics Platform (MBP) and co-director of the Imperial College Advanced Hackspace, a member of the steering committees for Agri-net, the Nutrition Food Network and the AgriFutures Lab at Imperial College London. He is Chair of the International Advisory Board for the SOFI CDT and a member of the advisory board for the BCFN CDT and Lab on a Chip journal. He is a leading specialist in biomembrane engineering, drug-membrane interactions, biomimicry, soft condensed matter, chemical biology, microfluidics, artificial cells, single cell analysis and lipid membrane mechanics, co-authoring > 100 papers in these fields. Since 2006 he has raised over £35 M in research funding with over £10 M in current funding. Much of this portfolio underpins active collaborations with industry (AstraZeneca plc, GSK plc, P&G plc, Syngenta plc).